

SENSITIVE SIMULTANEOUS DETERMINATION OF PARACETAMOL AND DICLOFENAC BASED ON Au NANOPARTICLES – FUNCTIONALIZED GRAPHENE/POLY (L-ARGININE) GLASSY CARBON ELECTRODE

ESMAIL AFSHAR, FAHIMEH JALALI*

Department of Chemistry, Razi University, 67346, Kermanshah, Iran

ABSTRACT

A voltammetric sensor was proposed for simultaneous determination of paracetamol and diclofenac based on poly (L-arginine)/Au-graphene nanocomposite film deposited on a glassy carbon electrode. Cyclic voltammetry showed that paracetamol and diclofenac provided well - defined oxidation peaks at +0.443 and +0.644 V, respectively. Experimental parameters, such as the concentration of L-arginine and number of potential cycles in electro-polymerization step, accumulation potential and time, and the pH of buffer solution were optimized. Under the optimized conditions, linear relationships between oxidation peak current and concentration in the range 0.5 – 50.0 μM for paracetamol, and 0.5 – 40.0 μM for diclofenac were obtained in linear sweep voltammetry regime. The limits of detection (LOD) for paracetamol and diclofenac were 0.04 and 0.08 μM , respectively. The fabricated electrode exhibited good reproducibility and stability. The proposed method was successfully applied to the assessment of low concentrations of paracetamol and diclofenac in spiked human blood serum samples with satisfactory results.

Keywords: Paracetamol, Diclofenac, Arginine, Au, Graphene, Modified electrode, Voltammetry

1. INTRODUCTION

Paracetamol, N-acetyl-*p*-aminophenol (PAR), is used in the symptomatic management of pain and fever. It is much safer than other non-steroidal anti-inflammatory drugs.¹ Diclofenac, [*o*-(2,6-dichloroanilino) phenyl] acetate (DCF), is a relatively safe and effective non-steroidal drug with pronounced anti-rheumatic, anti-inflammatory, analgesic and anti-pyretic properties,² which is widely used in the treatment of degenerative joint diseases and other arthritic conditions.³

Combination of PAR and DCF is a successful therapeutic, very useful in many specific conditions.⁴⁻⁷ The widespread use of this pharmaceutical association has stimulated the development of analytical methods for simultaneous determination of both compounds. Some of these methods for determination of PAR (and/or) DCF include TLC,⁸ HPLC,⁹⁻¹⁴ spectrophotometry,¹⁵ solid-phase spectrophotometry,¹⁶ capillary electrophoresis,^{17, 18} and supercritical-fluid chromatography.¹⁹ Chemometrics-assisted methods for the quantification of both drugs have also been reported.^{20, 21}

However, some of the above mentioned techniques are time-consuming and costly. Furthermore, some techniques require skilled operators and complicated instrumentations. Electrochemical methods, on the other hand, have attracted considerable attention due to the advantages of fast response, simple operation, high sensitivity, excellent selectivity, and real-time detection under in situ conditions.²² However, determination of PAR or DCF using unmodified electrodes is rare because of the weak electroactivity of these drugs. As a result, it is necessary to use proper materials for modification of the electrode in order to enhance the voltammetric response to these species.

Nobel metal nanomaterials are widely used in modified electrodes and electroanalytical investigations. These nanomaterials have suitable properties for constructing electrochemical sensing platforms such as, high sensitivity and selectivity to detect target molecules based on different analytical strategies.²³ Gold nanoparticles (AuNPs) due to their large surface area, biocompatibility and high electrical conductivity²⁴ have been widely employed as a modifier in voltammetry for analysis of various species.²⁵⁻²⁸

Graphene (GR), as a two dimensional and monoatomic thick building block, is a carbon allotrope which has received attention due to its fast electron transportation, high electrical conductivity, excellent mechanical flexibility and good biocompatibility.²⁹⁻³² Therefore, attractive nature of GR led to extensive concerns for its synthesis and applications. GR, by definition, is a single-layer, two-dimensional material, but GR samples with two or more but less than ten layers are equally interesting.

GR and metal nanomaterials can be combined in preparing electrochemical sensors. The unique two-dimensional structure of GR makes it extremely attractive as a support material for metal and metaloxide catalyst nanoparticles.^{33, 34, 35} GR-based hybrid materials have shown great versatility as enhanced electrode materials for electrochemical sensors and biosensors applications.^{36, 37} The combination of GR with AuNPs is one of the hot research topics due to its excellent conductivity and biocompatibility.³⁸⁻⁴⁰

In recent years, polymerization of amino acids has also attracted considerable attention in the field of electrochemical sensors due to their excellent electrocatalytic properties. Poly (L-arginine), poly (L-cysteine) and

other poly amino acids have been used for electrode modification, solely or in combination with other modifiers.⁴¹⁻⁴⁶ Chemical and electrochemical methods have been developed for the deposition of these polymers.

In the present study, poly (L-arginine), PAG, was electrodeposited on a glassy carbon electrode (GCE). GR was chemically functionalized with Au nanoparticles (AuNPs) and then drop - coated on PAG/GCE. The modified electrode showed electrocatalytic activity in the oxidation of PAR and DCF. To the best of our knowledge, there is no report on electrochemical simultaneous determination of these drugs. AuNPs-GR/PAG/GCE was successfully used in the determination of PAR and DCF in human blood serum samples.

2. EXPERIMENTAL

2.1. Reagents and solutions

PAR and DCF were kindly supplied by Tolid Daru Pharmaceutical Co. (Tehran, Iran) and used without further purification. All other chemicals were of analytical grade and used as received. Phosphate buffer solution (PBS, 0.1 M, pH 7.0) was used as supporting electrolyte in the present study. Stock solutions of PAR and DCF (1.0 mmol L⁻¹) were prepared by dissolving suitable amounts of solid standards in deionized water. These solutions were always stored in the refrigerator at 4–6 °C when not in use. More dilute solutions were freshly prepared by diluting the standard solution with PBS (0.1 mol L⁻¹, pH 7.0). Double distilled deionized water was used for preparation of all solutions.

2.2. Apparatus

Voltammetric measurements were carried out with a μ -Autolab (Utrecht, The Netherlands). The system was run using NOVA 1.8 software. The electrochemical cell was assembled with a Ag/AgCl/KCl, 3 mol L⁻¹ as reference electrode, a Pt wire as auxiliary electrode, and the prepared working electrodes. The surface morphology of modified electrodes was characterized by scanning electron microscopy, SEM (KYKY-EM 3200). A Jenway-3345 pH/Ion Meter (Dunmow, Essex) was used for pH measurements.

2.3. Preparation of GR-AuNPs nanocomposite

Graphene oxide (GO) was synthesized via the simplified Hummers method⁴⁷ in which a 9:1 sulfuric acid : phosphoric acid (360:40 mL) solution was prepared, into which 3 g of graphite powder was added. Potassium permanganate (18 g) was gradually added and the solution was left to oxidize for 3 days whilst being continuously stirred. After 3 days, the resulting solution was cooled to room temperature and poured onto ice (~400 mL) along with addition of 27 mL of hydrogen peroxide (30%). The solution was centrifuged and washed three times with 1 M of HCl aqueous solution and repeatedly with deionized water. The final GO dispersion was light brown in color.

In order to prepare Gr-AuNPs nanocomposite⁴⁸, NaOH (35 mg) was added into 10 mL of GO solution (1 mg GO mL⁻¹ water). After ultrasonication for 30 min, 418 μL of HAuCl₄ aqueous solution (10 mg/mL) was added and the mixture was stirred for 12 h at 80 °C. Afterwards, hydrazine (6 mL, 85%) was introduced under stirring and the solution was kept at 80 °C for 24 h. The product was then centrifuged, washed with water and ethanol for three times, and then the formed Gr-AuNPs nanocomposite was dissolved in 10 mL of deionized water.

2.4. Fabrication of modified electrode

Prior to the fabrication process, the bare GCE was well polished with 0.05 μm alumina slurry and sonicated in ethanol to remove the alumina particles. GCE was then washed with deionized water and dried in air. The electrode was immersed in PBS (0.1 M, pH 7.0) contained L-arginine (AG, 1.0 mM). Cyclic voltammetry (CV) was performed in potential range $-2 - 2.5$ V at a scan rate of 100 mV s^{-1} (6 cycles). As is well known, AG monomer could be oxidized to form α -amino free radical at high positive potentials, which can be linked to the electrode surface⁴⁹. PAG could be obtained by reaction between $-\text{NH}_2$ and $-\text{COOH}$ groups of adjacent molecules by liberating a water molecule.

The obtained PAG - modified GCE was washed with deionized water and dried in air for a few minutes. Finally, AuNPs-GR/PAG/GCE was prepared by dropping the suspension of GR-AuNPs (3 μL) on the PAG/GCE surface using a micro syringe, and then dried in air. Prior to use, AuNPs-GR/PAG/GCE was pretreated by cyclic voltammetry (10 cycles) between 0.0 and 1.0 V in PBS (0.1 mol L^{-1} , pH 7.0).

2.4. Analytical procedures and analysis of human serum sample

Anodic stripping voltammetry was employed to investigate the electrochemical behavior or quantification of PAR and DCF compounds. Individual and simultaneous analytical curves were obtained by addition of aliquots of PAR and DCF standard solutions into the electrochemical cell containing 10.0 mL of PBS (0.1 mol L^{-1} , pH 7.0). The detection limit was calculated as three times the standard deviation for the blank solution divided by the slope of the analytical curve. All the voltammetric experiments were carried out at ambient temperature of $25^\circ\text{C} \pm 2^\circ\text{C}$.

Healthy blood serum samples were obtained from a local pathology clinic and stored under refrigeration. For 1 mL blood sample, 0.15 mL perchloric acid was added, vortex-mixed for 1 min and centrifuged at 2500 rpm for 15 min. And then, 100 μL of supernatant (almost free from proteins) was added to PBS (0.1 mol L^{-1} , pH 7.0) to get a total volume of 10 mL for the drug determination in human serum.

3. RESULTS AND DISCUSSION

3.1. SEM characterization

Figure 1 shows the SEM image of the prepared AuNPs-GR/PAG/GCE, displaying clearly flexible GR sheets on the PAG film. The integration between AuNPs and GR can be visualized from the SEM image, in which Au nanoparticles at the size of 29–50 nm are embedded on the GR sheets. AuNPs distributed on the GR sheets may provide a large available surface area and largely enhanced electrical conductivity of the sensor.

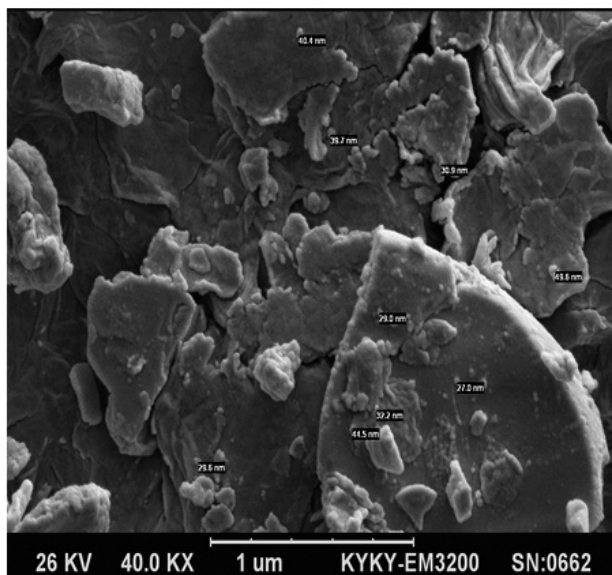


Figure 1 SEM image of AuNPs-GR/PAG/GCE.

3.2. Electrochemical behavior of PAR and DCF at different electrodes

The sensitive electrochemical detection of PAR and DCF on unmodified electrodes such as GCE is difficult, because currents are low (Fig. 2, curve a). At GCE, PAR (20.0 $\mu\text{mol L}^{-1}$) showed a broad irreversible oxidation peak

at 0.43 V and a very small cathodic peak at 0.34 V, in which the separation between the anodic and cathodic peak potentials was approximately 0.09 V. Moreover, DCF (35.0 $\mu\text{mol L}^{-1}$) demonstrated only an oxidation peak at 0.636 V without any cathodic counterpart, in agreement with previously report.⁵⁰ It was concluded that the electrochemical reactions of these species at unmodified GCE was irreversible, indicating the sluggish electron transfer kinetics of these compounds.

At AuNPs-GR/GCE (curve b), PAR showed an anodic peak (0.49 V) and a very small cathodic peak (0.23 V), whereas the anodic peak for DCF occurred at 0.65 V. Compared to unmodified GCE (curve a), these potentials were shifted to more positive values. The peak currents (i_{pa}), however, were increased (14.64 and 1.17 times higher than those at GCE, for PAR and DCF, respectively), confirming the more sensitivity of AuNPs-GR/GCE for PAR compared to DCF.

At PAG/GCE (curve c), PAR showed a pair of well-defined redox peaks with anodic and cathodic peak potentials at 0.413 and 0.382 V, respectively ($\Delta E = 0.031$ V), which showed considerable negative shift compared to unmodified and AuNPs-GR/GCE electrodes. DCF demonstrated an oxidation peak at 0.624 V. Significant increase in peak currents of both drugs at PAG/GCE (57.8 and 46.8 times more than those at GCE for PAR and DCF, respectively) showed the great electrocatalytic effect of PAG.

The cyclic voltammogram of PAR and DCF at AuNPs-GR/PAG/GCE (curve d) shows the largest oxidation peak currents, which are 94.2 and 47.1 times as high as those at GCE, respectively. In addition, the oxidation peak potentials on AuNPs-GR/PAG/GCE shift slightly to more positive potential compared to PAG/GCE. Moreover, the peak potential difference of about 0.201 V between the oxidation peaks clearly allows the simultaneous determination of both drugs on the modified electrode. These results might be attributed to the synergistic effect of PAG and AuNPs-GR, in which PAG has electrocatalytic activity for the two compounds and AuNPs-GR provide a large specific surface area.

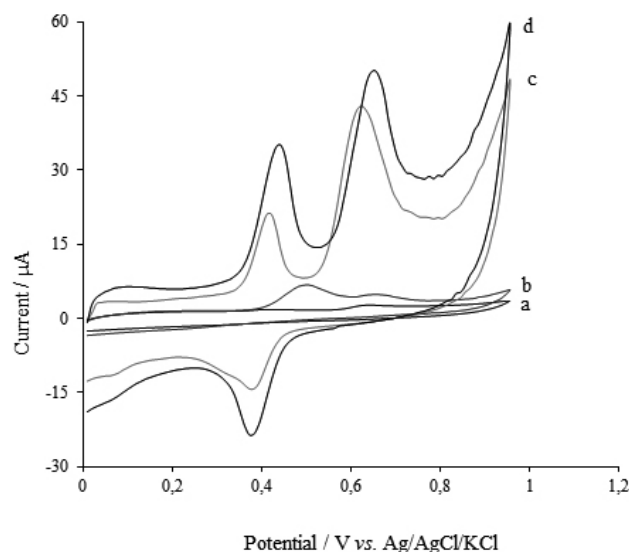


Figure 2 Cyclic voltammetry of PAR (20.0 $\mu\text{mol L}^{-1}$) and DCF (35.0 $\mu\text{mol L}^{-1}$) at four different electrodes: (a) GCE, (b) AuNPs-GR/GCE, (c) PAG/GCE and (d) AuNPs-GR/PAG/GCE. Voltammetric conditions: buffer solution: PBS (0.1 mol L^{-1} , pH 7.0), v : 100 mV s^{-1} .

The kinetics of the electrode reactions was investigated by studying the effect of potential sweep rate (v) on the anodic peaks. Cyclic voltammograms of a mixture of PAR (7.0 $\mu\text{mol L}^{-1}$) and DCF (10.0 $\mu\text{mol L}^{-1}$) in PBS (pH 7.0) were recorded at AuNPs-GR/PAG/GCE by increasing scan rate from 10 to 350 mV s^{-1} (Fig. 3A). The results showed that both anodic peak currents increased linearly with the scan rate (Fig. 3B), confirming the adsorption-controlled process for electro-oxidation of PAR and DCF. The linear regression equations were:

$$\text{PAR: } i_{pa} = 0.1656 v - 2.7204 \quad (r^2 = 0.9939)$$

$$\text{DCF: } i_{pa} = 0.0999 v + 0.0025 \quad (r^2 = 0.9981)$$

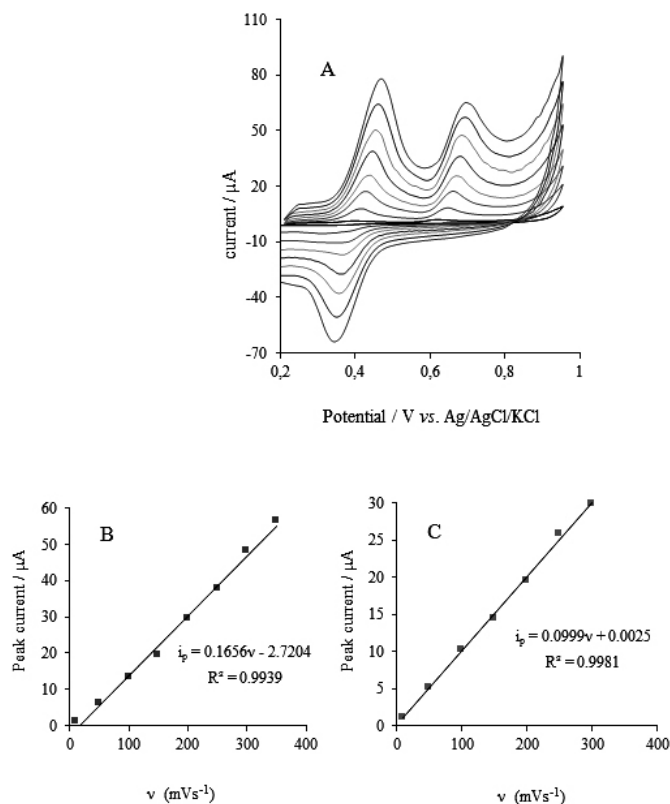


Figure 3 (A) Cyclic voltammetry of PAR (7.0 μmol L⁻¹) and DCF (10.0 μmol L⁻¹) on AuNPs-GR/PAG/GCE in PBS (0.1 mol L⁻¹, pH 7.0) at various scan rates; from inner to outer: scan rates of 10, 50, 100, 150, 200, 250, 300, and 350 mV s⁻¹ (B) Variation of i_{pa} vs. v for PAR and (C) Variation of i_{pa} vs. v for DCF.

3.3. Optimization of parameters affecting the determination of PAR and DCF

3.3.1. Modification of the electrode

Concentration of AG and the number of cycles in electro-polymerization step

The concentration of AG is an important factor in the polymerization step, due to its determinant effect on the polymeric film thickness, so on the conductivity of the electrode. Electro-polymerization of AG was carried out in different concentrations of the amino acid (0.5 – 3.0 mmol L⁻¹), and the voltammetric responses of PAR (8.0 μmol L⁻¹) and DCF (8.0 μmol L⁻¹) were recorded. (Fig. 4A). The peak currents of the drugs enhanced up to AG concentration of 1.0 mmol L⁻¹. At higher concentrations of AG, the peak currents decreased, probably due to the blocking effect of thicker poly- AG (PAG) film.

The number of potential cycles used in electropolymerization was also effective on the deposited polymer thickness. The anodic currents of PAR and DCF rose up to 6 cycles and then decreased (Fig. 4B). The phenomenon could be associated with the increasing thickness of the polymeric film, which hindered the transfer of electrons on the electrode surface.

3.3.2. Experimental conditions for PAR and DCF analysis at AuNPs-GR/PAG/GCE

Accumulation potential and preconcentration time

From the study of scan rate, the adsorptive nature of current was proposed, therefore, the potential and duration of adsorption had to be investigated. The potential of AuNPs-GR/PAG/GCE, on which the drugs were adsorbed, was changed from -0.2 to 0.2 V against Ag/AgCl/KCl (3 mol L⁻¹). The oxidation peak currents of PAR and DCF (each 10 μmol L⁻¹) attained maximal values as the accumulation potential was 0.0 V. For further studies, the potential of 0.0 V was applied in the accumulation step. Next, the preconcentration time was changed in the range from 0 to 180 s and its influence on the oxidation peaks of PAR and DCF was studied. After preconcentration for 120 s, the largest peak currents for the drugs were obtained during cyclic voltammetry.

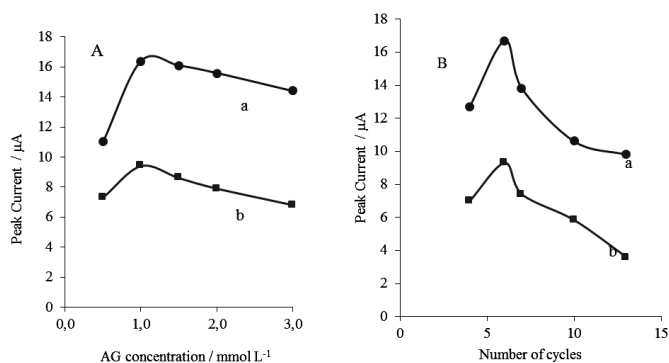


Figure 4 Optimization of conditions for electrode modification. (A) Effect of L-arginine concentration on electrode response towards PAR (a) and DCF (b); (B) The effect of number of potential cycles towards PAR (a) and DCF (b). [PAR] = [DCF] = 8.0 μmol L⁻¹, PBS (0.1 mol L⁻¹, pH 7), $v = 100$ mV s⁻¹.

Effect of pH

The effect of solution pH on oxidation peak potentials and currents of PAR and DCF was studied at AuNPs-GR/PAG/GCE. The anodic peak potentials of the drugs were decreased linearly as the pH was increased from 4.0 to 10.0. Linear regression equations $E_{pa} = -0.0555 \text{ pH} + 0.8501$ and $E_{pa} = -0.0404 \text{ pH} + 0.9568$ (Fig. 5A) were obtained for PAR and DCF, respectively, demonstrating that equal numbers of electrons and protons were involved in the oxidation processes. The oxidation mechanism of PAR and DCF has been extensively investigated in the literature which shows participation of 2 e⁻ and 2 H⁺.⁵¹⁻⁵⁸

Oxidation peak currents of PAR and DCF were also affected by solution pH (Fig. 5B). Within the pH range of 4.0 – 10.0, the anodic peak currents increased from pH 4.0 to 7.0 and then decreased at higher pH values. Therefore, considering the sensitivity, PBS (0.1 M, pH 7.0) was chosen as supporting electrolyte for the simultaneous determination of PAR and DCF in this study.

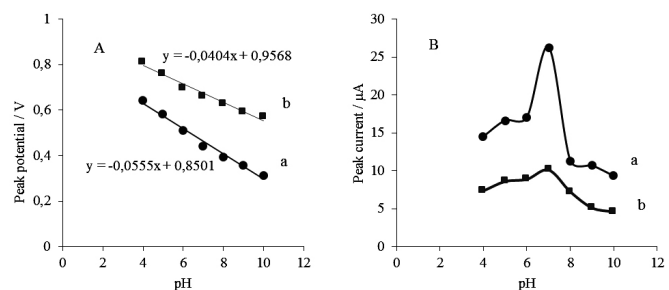


Figure 5 Influence of pH on (A) peak potentials and (B) peak currents. Scan rate: 100 mV s⁻¹. PAR (a) and DCF (b).

3.4. Determination of PAR and DCF

Linear sweep voltammetry (LSV) was used for separate or simultaneous determination of PAR and DCF at AuNPs-GR/PAG/GCE. In order to study the probable interference of the presence of DCF on PAR determination (or vice versa), two different experiments were carried out under optimized conditions in PBS (pH 7.0). In each experiment, the concentration of one of the compounds was varied while keeping the concentration of the other compound constant. The variation in PAR concentration (0.0 – 30.0 μmol L⁻¹) in the presence of a constant amount of DCF (10.0 μmol L⁻¹) obviously showed no interference (Fig. 6A). While the oxidation peak current of PAR increased linearly with concentration, the peak current of DCF was almost constant. A similar experiment was repeated, by varying the concentration of DCF in the presence of a constant amount of PAR (Fig. 6B), which demonstrated the independence of DCF determination from the presence of PAR.

Simultaneous determination of PAR and DCF was studied by changing the concentrations of both drugs and recording LSVs (Fig. 7A). The calibration graph for PAR consisted of two linear segments (Fig. 7B) with linear regression equations of $i_{pa} = 1.8274 [\text{PAR}] + 1.33$ ($R^2 = 0.992$) and $i_{pa} = 0.55 [\text{PAR}] + 15.14$ ($R^2 = 0.997$) in the whole concentration range of 0.5–50.0 μmol L⁻¹.

The calibration graph for DCF presented a linear response in the concentration range 0.5–40.0 $\mu\text{mol L}^{-1}$ (Fig. 7C) with linear regression equation of $i_{pa} = 0.7791 [\text{DCF}] + 2.319$ ($R^2 = 0.996$). Detection limits (LODs) of the method were calculated as 0.04 and 0.08 $\mu\text{mol L}^{-1}$ for PAR and DCF, respectively.

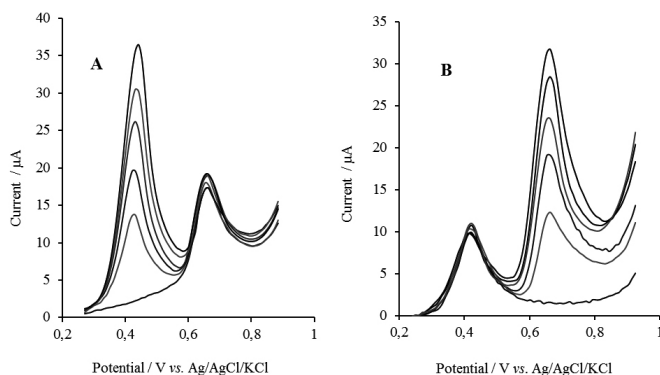


Figure 6 (A) LSV curves of AuNPs-GR/PAG/GCE at different concentrations of PAR (0.0–30.0 $\mu\text{mol L}^{-1}$) and constant concentration of DCF (10.0 $\mu\text{mol L}^{-1}$); (B) LSV curves at different concentration of DCF (0.0–30.0 $\mu\text{mol L}^{-1}$) and constant concentration of PAR (5.0 $\mu\text{mol L}^{-1}$). Supporting electrolyte: PBS (0.1 mol L^{-1} , pH 7.0) and scan rates: 100 mV s^{-1} .

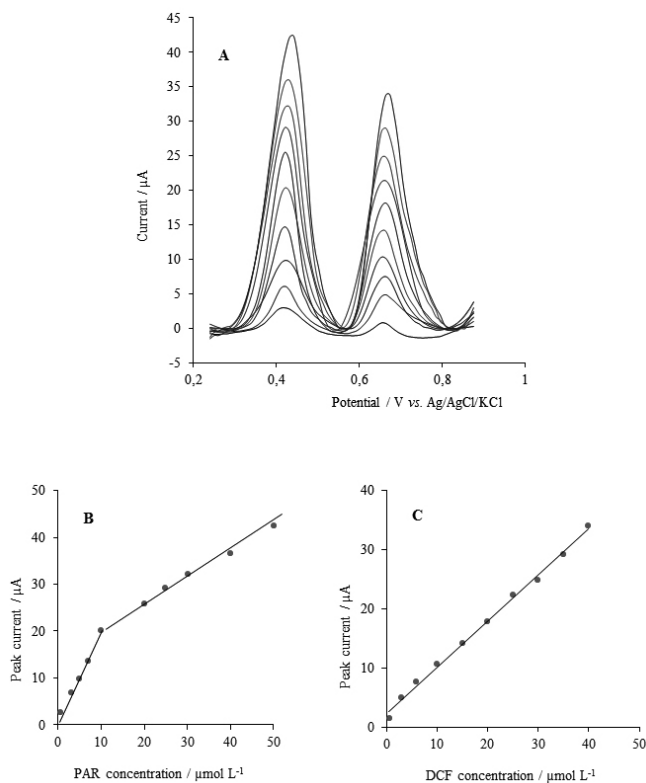


Figure 7. (A) LSV curves obtained for the simultaneous oxidation of PAR and DCF. [PAR] = 0.5–50.0 $\mu\text{mol L}^{-1}$ for and [DCF] = 0.5–40.0 $\mu\text{mol L}^{-1}$; Calibration curves for (B) PAR and (C) DCF. Supporting electrolyte: PBS (0.1 mol L^{-1} , pH 7.0) and scan rates: 100 mV s^{-1} .

The results of the present study were compared with some of similar reported methods for the determination of PAR or DCF (Table 1). The linear ranges and LODs for PAR and DCF observed at AuNPs-GR/PAG/GCE are comparable with those obtained for some of the other modified electrodes, besides the simultaneous determination in the present method.

3.5. Interference study

The influence of some coexistent substances was examined in the determination of PAR and DCF by the proposed method. The selected inorganic ions and organic compounds commonly exist in pharmaceuticals and biological samples.

The tolerance limit was set as the amount of foreign species causing $\pm 10\%$ error in determination of PAR (10.0 $\mu\text{mol L}^{-1}$) and DCF (15.0 $\mu\text{mol L}^{-1}$). The results showed that over 1000-fold excess concentration of Na^+ , Ca^{2+} , K^+ and over 500-fold glucose, valine, glycine, urea and 30-fold ascorbic acid did not interfere with the PAR and DCF analysis (signal changes for these species were less than $\pm 7\%$). The obtained results showed the satisfactory selectivity of the proposed composite electrode even in the presence of high concentrations of other species.

3.6. Repeatability, Reproducibility, and stability of the modified electrode

The repeatability of the method was examined and the relative standard deviation (RSD%) for seven successive assays was 1.3% and 1.8% for PAR (10 $\mu\text{mol L}^{-1}$) and DCF (15 $\mu\text{mol L}^{-1}$), respectively. The reproducibility of five different fabricated electrodes was investigated in PBS (0.1 M, pH 7.0) containing PAR and DCF, and RSD% were found to be less than 5.3%. After the electrode was stored for 7 days at ambient temperature, the oxidative peak currents (LSV) reduced less than 4.8%. These results indicated that AuNPs-GR/PAG/GCE has good stability and reproducibility, and could be used for accurate and precise PAR and DCF detection.

3.7. Application of the proposed method in real samples

Blood plasma concentrations of PAR between 10–20 $\mu\text{g/mL}$ (66–132 μM) are known to produce an antipyretic effect.⁵⁹ In the case of DCF, in fasting subjects, the mean peak plasma concentration of 1.5 $\mu\text{g/mL}$ (5 μM) is attained on average 2 hours after ingestion of one tablet of 50 mg. Suppositories of 50 mg produce a corresponding mean peak plasma concentration of 1.2 $\mu\text{g/mL}$ (4 μM).⁶⁰ In order to demonstrate the ability of the modified electrode for real sample analysis, PAR and DCF were spiked to human blood serum sample (in therapeutic range). The recoveries clearly demonstrated that the sensor gave high selectivity, accuracy, and good reproducibility in the voltammetric determination of PAR and DCF (Table 2), implying that the proposed modified electrode has capability for real sample analysis without considerable error.

4. CONCLUSIONS

The present study showed the successful application of AuNPs-GR/PAG/GCE in the simultaneous determination of PAR and DCF. Low LODs were obtained in simultaneous analytical assays for both drugs. Moreover, AuNPs-GR/PAG/GCE showed significant sensitivity, repeatability, and precision. Under optimized conditions, the modified electrode showed wide linear concentration ranges of 0.5 – 50.0 $\mu\text{mol L}^{-1}$ and 0.5 – 40.0 $\mu\text{mol L}^{-1}$ with LODs 0.04 and 0.8 $\mu\text{mol L}^{-1}$ for PAR and DCF, respectively. Finally, the proposed method was applied to simultaneous determination of micro molar concentrations of PAR and DCF in human blood serum samples with recoveries ranging from 97.5 to 103.0%.

Table 1. Comparison of some characteristics of different modified electrodes for the determination of PAR and DCF

Method	Linear Range (μM)		LOD (μM)		In the presence of other analytes	Ref.
	PAR	DCF	PAR	DCF		
SWV	5.0 – 500	–	–	–	Tryptophan and Isoproterenol Tramadol Norepinephrine and L-tyrosine Pyridoxine Codeine Glutathione	61
SWV	0.01 – 9.0	–	1.0	–		62
DPV	1.9 – 188	–	0.0036	–		63
DPV	188	–	0.1	–		64
SWV	25.0 – 150	–	4.3	–		65
SWV	0.03 – 12.0	–	0.5	–		66
SWV	0.8 – 600	–	–	–		
SWV	0.02 – 140	–	0.009	–	Ascorbic acid and Tryptophan Alone	67
SWV	–	0.3 – 750	–	0.09		68
DPV	–	0.5 – 300	–	0.2	Alone	69
SWV	–	5.0 – 600	–	2.0	Morphine Alone	50
DPV	–	10.0 – 140	–	3.28	Alone	56
SWV	–	0.01 – 1.0	–	0.0062	Alone	
DPV	–	0.05 – 50.0	–	0.018	Indomethacin	70
LSV	0.5 – 50.0	0.5 – 40.0	0.04	0.08		–

Table 2. Determination of PAR and DCF in a blood serum sample ($n = 3$)^a.

Added (μM)		Found (μM)			% Recovery	
PAR	DCF	PAR	DCF	PAR	DCF	
		1.95 (± 0.03)				
2.0	2.0	3.07 (± 0.03)	1.97 (± 0.04)		97.5	98.5
3.0	3.0	4.21 (± 0.06)	3.02 (± 0.04)		102.3	100.7
4.0	4.0	5.08 (± 0.05)	4.12 (± 0.08)		105.2	103.0
5.0	5.0		4.94 (± 0.06)		101.6	98.8

^a Average of three replicate determinations.

REFERENCE

- Ellis, M.; Haydik, I.; Gillman, S.; Cummins, L.; Cairo, M. S.; *J. Pediatr.*, **114**, 654 (1989).
- Small, R.; *Clin. Pharm.*, **8**, 545 (1989).
- Crowley, B.; Hamill, J.; Lyndon, S.; McKellian, J.; Williams, P.; Miller, A.; *Curr. Med. Res. Opin.*, **12**, 143 (1990).
- Ward, M.; Kirwan, J.; Norris, P.; Murray, N.; *Rheumatology*, **25**, 412 (1986).
- Hiller, A.; Silvanto, M.; Savolainen, S.; Tarkkila, P.; *Acta Anaesthesiol. Scand.*, **48**, 1185 (2004).
- Breivik, E. K.; Barkvoll, P.; Skovlund, E.; *Clin. Pharmacol. Ther.*, **66**, 625 (1999).
- Matthews, R.; Scully, C.; Levers, B.; *Br. Dent. J.*, **157**, 357 (1984).
- Shinde, V.; Tendolkar, N.; Desai, B.; *JPC. J. planar chromatogr., modern TLC*, **7**, 50 (1994).
- Siddiqui, F. A.; Arayne, M. S.; Sultana, N.; Qureshi, F.; *J. AOAC Int.*, **94**, 150 (2011).
- Jana, K.; Adhikari, L.; Motira, S.; Behera, A.; *Asian J. Pharmaceut. Clinic. Res.*, **4**, 41 (2011).
- Hafsa, D.; Chanda, S.; J Prabhu, P.; *J. Chem.*, **8**, 1620 (2011).
- Badgujar, M. A.; Pingale, S. G.; Mangaonkar, K. V.; *J. Chem.*, **8**, 1206 (2011).
- Biswas, A.; Basu, A.; *International Journal of Pharma & Bio Sciences*, **1**, (2010).
- Gowramma, B.; Rajan, S.; Muralidharan, S.; Meyyanathan, S.; Suresh, B.; *Inter. J. ChemTech Res.*, **2**, 676 (2010).
- Souza, R. L. d.; Tubino, M.; *J. Braz. Chem. Soc.*, **16**, 1068 (2005).
- Fernández de Córdova, M.; Ortega Barrales, P.; Molina Díaz, A.; *Anal. Chim. Acta*, **369**, 263 (1998).
- Solangi, A.; Memon, S.; Mallah, A.; Memon, N.; Khuhawar, M. Y.; Bhangar, M. I.; *Turk. J. Chem.*, **34**, 921 (2010).
- Solangi, A. R.; Memon, S. Q.; Mallah, A.; Memon, N.; Khuhawar, M. Y.; Bhangar, M. I.; *Pak. J. Pharm. Sci.*, **24**, 539 (2011).
- Patil, S. T.; Sundaresan, M.; Bhoir, I. C.; Bhagwat, A.; *Talanta*, **47**, 3 (1999).
- Castellano, P. M.; Vignaduzzo, S. E.; Maggio, R. M.; Kaufman, T. S.; *Anal. Bioanal. Chem.*, **382**, 1711 (2005).
- Balamurugan, C.; Aravindan, C.; Kannan, K.; Sathyanarayana, D.; Valliappan, K.; Manavalan, R.; *Indian J. Pharm. Sci.*, **65**, 274 (2003).
- Rogers, K. R.; Becker, J. Y.; Wang, J.; Lu, F.; *Field Anal. Chem. & Technol.*, **3**, 161 (1999).
- Guo, S.; Wang, E.; *Nano Today*, **6**, 240 (2011).
- Xu, S.; Han, X.; *Biosens. Bioelectron.*, **19**, 1117 (2004).
- Villalonga, R.; Diez, P.; Yáñez-Sedeño, P.; Pingarrón, J. M.; *Electrochim. Acta*, **56**, 4672 (2011).

26. Li, J.; Xie, H.; Chen, L.; *Sensor. Actuat. B*, **153**, 239 (2011).
27. Li, F.; Feng, Y.; Dong, P.; Yang, L.; Tang, B.; *Biosens. Bioelectron.*, **26**, 1947 (2011).
28. Daniel, M.-C.; Astruc, D.; *Chem. Rev.*, **104**, 293 (2004).
29. Zhang, X.; Yin, J.; Peng, C.; Hu, W.; Zhu, Z.; Li, W.; Fan, C.; Huang, Q.; *Carbon*, **49**, 986 (2011).
30. Lee, C.; Wei, X.; Kysar, J. W.; Hone, J.; *Science*, **321**, 385 (2008).
31. Balandin, A. A.; Ghosh, S.; Bao, W.; Calizo, I.; Teweldebrhan, D.; Miao, F.; Lau, C. N.; *Nano Lett.*, **8**, 902 (2008).
32. Novoselov, K. S.; Geim, A. K.; Morozov, S.; Jiang, D.; Zhang, Y.; Dubonos, S.; Grigorieva, I.; Firsov, A.; *Science*, **306**, 666 (2008).
33. Wang, S.; Wang, X.; Jiang, S. P.; *PCCP*, **13**, 6883 (2011).
34. Han, F.; Wang, X.; Lian, J.; Wang, Y.; *Carbon*, **50**, 5498 (2012).
35. Kamat, P. V.; *J. Phys. Chem. Lett.*, **1**, 520 (2009).
36. Shan, C.; Yang, H.; Han, D.; Zhang, Q.; Ivaska, A.; Niu, L.; *Biosens. Bioelectron.*, **25**, 1070 (2010).
37. Guo, S.; Wen, D.; Zhai, Y.; Dong, S.; Wang, E.; *ACS Nano*, **4**, 3959 (2010).
38. Muszynski, R.; Seger, B.; Kamat, P. V.; *J. Phys. Chem. C*, **112**, 5263 (2008).
39. Sanghavi, B. J.; Kalambate, P. K.; Karna, S. P.; Srivastava, A. K.; *Talanta*, **120**, 1 (2014).
40. Er, E.; Çelikkan, H.; Erk, N.; Aksu, M. L.; *Electrochim. Acta*, **157**, 252 (2015).
41. Cao, Q.; Zhao, H.; Yang, Y.; He, Y.; Ding, N.; Wang, J.; Wu, Z.; Xiang, K.; Wang, G.; *Biosens. Bioelectron.*, **26**, 3469 (2011).
42. Vilian, A. E.; Chen, S.-M.; *RSC Advances*, **4**, 50771 (2014).
43. Ma, W.; Sun, D.-M.; *Chinese J. Anal. Chem.*, **35**, 66 (2007).
44. Zhang, K.; Luo, P.; Wu, J.; Wang, W.; Ye, B.; *Anal. Method.*, **5**, 5044 (2013).
45. Santos, D. P.; Bergamini, M. F.; Fogg, A. G.; Zannoni, M. V. B.; *Microchim. Acta*, **151**, 127 (2005).
46. Devadas, B.; Cheemalapati, S.; Chen, S.-M.; Ali, M. A.; Al-Hemaid, F. M.; *Ionics*, **1** (2014).
47. Huang, N. M.; Lim, H.; Chia, C.; Yarmo, M.; Muhamad, M.; *Inter. J. Nanomed.*, **6**, 3443 (2011).
48. Zhao, L.; Zhao, F.; Zeng, B.; *Int. J. Electrochem. Sci*, **9**, 1366 (2014).
49. Jiang, C.; Yang, T.; Jiao, K.; Gao, H.; *Electrochim. Acta*, **53**, 2917 (2008).
50. Chethana, B.; Basavanna, S.; Arthoba Naik, Y.; *Ind. Eng. Chem. Res.*, **51**, 10287 (2012).
51. Habibi, B.; Jahanbakhshi, M.; Pournaghi-Azar, M. H.; *Anal. Biochem.*, **411**, 167 (2011).
52. Nematollahi, D.; Shayani-Jam, H.; Alimoradi, M.; Niroomand, S.; *Electrochim. Acta*, **54**, 7407 (2009).
53. Li, C.; Zhan, G.; Yang, Q.; Lu, J.; *Bull. Korean Chem. Soc*, **27**, 1854 (2006).
54. Kumar, S. A.; Tang, C.-F.; Chen, S.-M.; *Talanta*, **76**, 997 (2008).
55. Ghorbani-Bidkorbeh, F.; Shahrokhian, S.; Mohammadi, A.; Dinarvand, R.; *Electrochim. Acta*, **55**, 2752 (2010).
56. Goyal, R. N.; Chatterjee, S.; Agrawal, B.; *Sensor. Actuat. B: Chem.*, **145**, 743 (2010).
57. Arvand, M.; Gholizadeh, T. M.; Zanjanchi, M. A.; *Mater. Sci. Engin.: C*, **32**, 1682 (2012).
58. Goodarzi, M.; Khalilzade, M. A.; Karimi, F.; Kumar Gupta, V.; Keyvanfard, M.; Bagheri, H.; Fouladgar, M.; *J. Mol. Liq.*, **197**, 114 (2014).
59. Rumack, B. H.; *Pediatrics*, **62**, 943 (1978).
60. Vignoni, A.; Fierro, A.; Moreschini, G.; Cau, M.; Agostino, A.; Daniele, E.; Foti, G.; Grossi, E.; *J. Int. Med. Res.*, **11**, 303 (1983).
61. Karimi-Maleh, H.; Moazampour, M.; Ahmar, H.; Beitollahi, H.; Ensafi, A. A.; *Measurement*, **51**, 91 (2014).
62. Afkhami, A.; Khoshsafar, H.; Bagheri, H.; Madrakian, T.; *Anal. Chim. Acta*, **831**, 50 (2014).
63. Taei, M.; Ramazani, G.; *Colloid. Surf. B*, **123**, 23 (2014).
64. Barsan, M. M.; Toledo, C. T.; Brett, C. M.; *J. Electroanal. Chem.*, (2014).
65. Afkhami, A.; Khoshsafar, H.; Bagheri, H.; Madrakian, T.; *Sensor. Actuat. B*, **203**, 909 (2014).
66. Shahmiri, M. R.; Bahari, A.; Karimi-Maleh, H.; Hosseinzadeh, R.; Mirnia, N.; *Sensor. Actuat. B*, **177**, 70 (2013).
67. Keyvanfard, M.; Shakeri, R.; Karimi-Maleh, H.; Alizad, K.; *Mater. Sci. Engin.: C*, **33**, 811 (2013).
68. Ensafi, A. A.; Izadi, M.; Karimi-Maleh, H.; *Ionics*, **19**, 137 (2013).
69. Mokhtari, A.; Karimi-Maleh, H.; Ensafi, A. A.; Beitollahi, H.; *Sensor. Actuat. B*; **169**, 96 (2012).
70. Sarhangzadeh, K.; Khatami, A. A.; Jabbari, M.; Bahari, S.; *J. Appl. Electrochem.*, **43**, 1217 (2013).